JOURNAL OF CATALYSIS **61**, 48–56 (1980)

Thermal Desorption Study of Formic Acid Decomposition on a Clean Cu(110) Surface

DAVID H. S. YING AND ROBERT J. MADIX

Department of Chemical Engineering, Stanford University, Stanford, California 94305

Received July 20, 1978; revised June 1, 1979

The catalytic decomposition of formic acid was studied on a (110)-oriented copper single-crystal surface. Dehydrogenation of formic acid was the *sole* decomposition path observed. The parent molecule dissociated to form a stable formate species ($HCOO_{(a)}$) as the surface intermediate. It was postulated that the formate species was bonded to the surface copper sites through the two oxygen atoms. The decomposition of the formate species was the rate-limiting step governing the rates of the formation of the CO_2 and H_2 products. The rate constant was determined to be 9.4×10^{13} $\exp(-31{,}870/RT)$ $\sec^{-1}$. A comparison of the catalytic properties of the Cu(110) surface with those of the carburized Ni(110) surface showed strong chemical similarities between the two surfaces.

INTRODUCTION

The catalytic decomposition of formic acid on copper has been widely studied (*1–10*). It was generally agreed among most investigators that the dehydrogenation of formic acid was the predominant decomposition path. However, the activation energy for the decomposition of formic acid on copper catalysts reported in the literature showed the usual wide spread (from 8.5 to 36 kcal/mole). Recently Joyner and Roberts (*11*) used photoelectron spectroscopy to study the adsorption and catalytic decomposition of formic acid on polycrystalline copper in a temperature range of 80 to 500°K. The authors reported that at 80°K the adsorbed formic acid molecules were hydrogen-bonded to each other. This hydrogen-bonding broke up above about 140°K. Then between 170 and 190°K, reorientation of the formic acid molecule occurred, and it began to dissociate into a formate ion. The formate ion was held on the copper surface until above 400°K. The activation energy for the decomposition of the formate ion was measured to be 115–130 kJ/mole (27.5–31.1 kcal/mole) in a temperature range of 400–450°K by assuming a first-order process and assigning a value of 10^{13} for the preexponential factor.

In the present work, flash desorption spectroscopy was used to investigate the catalytic decomposition of formic acid on a clean Cu(110) single-crystal surface. One purpose of this study was to determine the decomposition mechanism and the kinetics of the reaction quantitatively in order to compare with previous results on nickel, and copper–nickel alloys. In addition, it has been suggested by McCarty and Madix (*12, 13*) that the nickel carbide surface may behave chemically more like copper than clean nickel. This suggestion followed that of Levi and Boudart (*14*) that transition metal carbides may have chemical properties similar to elements of higher atomic number in the same row of the periodic table. The other goal of the present study was to compare the catalytic properties of copper with those of the carburized Ni(110) surface (*12, 13*).

EXPERIMENTAL

The catalytic decomposition of formic acid on a clean Cu(110) single crystal surface was conducted in a stainless-steel ultrahigh vacuum reaction chamber. The reaction chamber was equipped with an argon ion bombardment gun, a UTI quadrupole mass spectrometer, four-grid

0021-9517/80/010048-09$02.00/0

LEED-Auger electronic optics, and a stainless-steel dosing needle. The arrangement of the equipment had been described previously (*15*). The pressure of the chamber was maintained in the 10^{-10} Torr region by means of a vac-ion pump and titanium sublimation pump.

The copper sample was (110)-oriented. The sample was initially cleaned by cycles of Argon ion sputtering at 300 V for 45 min and annealing at 925–950°K for 10 min. The cleanliness of the surface was measured by means of Auger electron spectroscopy. The major contaminants were S, C, and O. A clean sample surface was achieved when the Auger signals of these major contaminants were down to noise level. During the Auger measurement the sample was scanned to ensure cleanliness of the entire surface. A zigzag type of filament was made from a tungsten wire and located at the back of the copper sample. The area covered by the zigzag tungsten filament was comparable with that of the sample to provide even heating by radiation. The temperature of the sample was measured by a chromel-alumel thermocouple which was firmly held in a notch at the upper corner of the sample. The sample could be cooled to 173°K by means of a liquid nitrogen cooling tube.

The preparation and purification of the formic acid employed in the present study was described previously (*15*). The copper sample was maintained at a constant temperature before exposing to the formic acid vapor. This was achieved by adjusting the power input to the tungsten filament to partially compensate the cooling due to the liquid nitrogen cooling tube. The formic acid was kept at −45°C in a solid form, and its vapor was dosed on the copper sample through the stainless-steel dosing needle directed at the front face of the sample. The sample was flashed at a linear rate of 3.5 ksec^{-1} unless noted. The partial pressure rise of the products was measured by the mass spectrometer as a function of the sample temperature. The measured mass spectrometric signals directly represented their desorption rates because of the sufficiently high pumping speed of the system.

A shorthand notation $X(\beta)/Y$ was used to identify the desorption of the β state of gas X following the adsorption of gas Y. For example, $CO_2(\beta)/HCOOH$ refers to the β state of the CO_2 product following the adsorption of HCOOH. When the entire product spectrum was displayed the notation Prod/HCOOH was employed.

RESULTS

Formic Acid Decomposition

Formic acid adsorbed at 190°K with an initial sticking probability of unity. Saturation coverage near 2×10^{14} molecules/cm^2 was reached at an exposure of about 10^{15} molecules/cm^2 with the adsorption kinetics following *roughly* Langmuirian behavior. Extensive *condensed* layers were not formed at this temperature. Carbon dioxide and hydrogen were the sole product observed from the decomposition of formic acid on a Cu(110) surface. The produce distribution following the adsorption of HCOOH at 190°K is shown in Fig. 1. The $CO_2(\beta)$ and $H_2(\beta)$ products showed identical peak temperatures at 473°K with a heating rate of 3.4 ksec^{-1}. A mass 28 peak was observed at the same temperature which was totally accounted for by the cracking fraction of the $CO_2(\beta)$ product in the ionizer

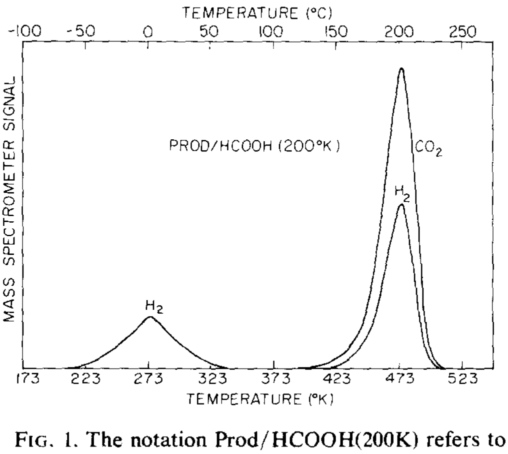

FIG. 1. The notation Prod/HCOOH(200K) refers to the product desorption spectrum subsequent to adsorption of HCOOH at 200°K.

of the mass spectrometer employed. When the adsorption temperature of the parent molecule was increased from 190 to 298°K, only the $CO_2(\beta)$ and $H_2(\beta)$ peaks were observed. The $H_2(\beta)/CO_2(\beta)$ ratio was calculated to be 0.4 ± 0.1. This stoichiometric ratio suggested the dissociative adsorption of the formic acid molecules at room temperature to form a stable surface intermediate with only one hydrogen atom. To within experimental error of about 20% this reaction occurred with a unit sticking probability. Small amounts of undissociated formic acid did desorb below room temperature.

When deuterated formic acid (HCOOD) was adsorbed at *room* temperature $CO_2(\beta)$ and $H_2(\beta)$ were the major decomposition products observed. As the adsorption temperature was lowered to 190°K, additional D_2 and HD products were detected. Figure 2 shows the product distribution following the adsorption of HCOOD at 190°K. The $CO_2(\beta)$ and $H_2(\beta)$ products showed identical peak position at 475°K as observed for the $CO_2(\beta)$/HCOOH and $H_2(\beta)$/HCOOH shown in Fig. 1, suggesting that formate is the stable surface intermediate. In addition, Fig. 2 shows a small $HD(\beta)$ peak and a $D_2(\beta)$ bump at 485 and 495°K, respectively, amounting to less than 10% of the $H_2(\beta)$ product. The evolution of these $HD(\beta)$ and $D_2(\beta)$ products was due to the DCOOD impurity in the HCOOD reactant gas, as inferred from the appearance of a small mass 48 signal in the mass scan of the HCOOD vapor. Furthermore, the major D_2 and HD products were detected below room temperature at 288 and 278°K, respectively. The evolution of $HD(\gamma)$ was undoubtedly due to HCOOH impurities in the dosed gas.

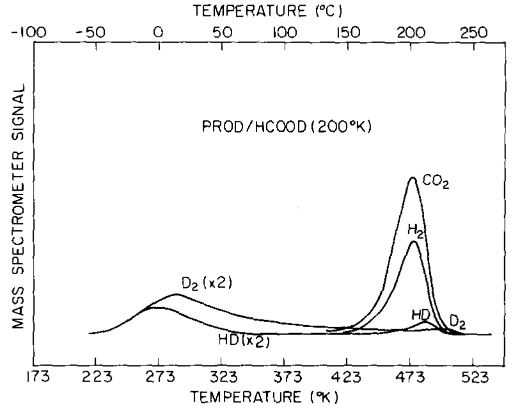

FIG. 2. Product distribution following the adsorption of HCOOD at 200°K. Heating rate was 3.4°K/sec.

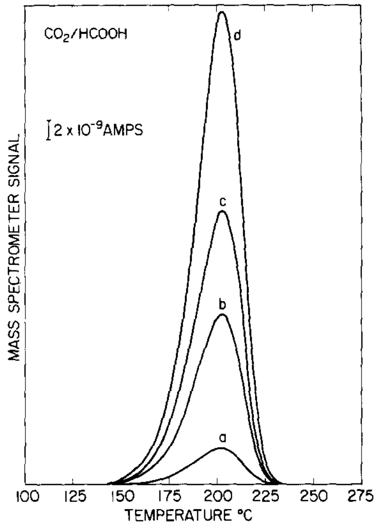

FIG. 3. A coverage variation study for the CO_2/HCOOH product peak. Relative exposures are given as pressure in the dosing line times the exposure time. (a) ≈100 μsec; (b) 500 μsec; (c) 2000 μsec; (d) 10000 μsec.

The CO_2 flash desorption spectra as a function of formic acid exposure are shown in Fig. 3. The CO_2 peak position was independent of formic acid exposure over two orders of magnitude change in the initial exposure. This constancy of the CO_2 peak temperature indicated a first-order process.

An isothermal technique was also employed to determine the reaction order for the CO_2 product. Equation (1),

$$N = kC^n, \qquad (1)$$

is a simple rate expression where N is the desorption rate, k is the rate constant, C is the surface concentration, and n is the reaction order. Since the rate constant k was assumed to be only temperature dependent, k will be a constant at a fixed temperature. Then a plot of $\ln(N)$ as a function of $\ln(C)$ at constant temperature should yield a straight line with slope representing the reaction order. Figure 4 shows a ln–ln plot of the CO_2 desorption rate versus the surface concentration. Four isotherms were used, covering the entire CO_2 flash desorption spectrum. The values of these slopes are shown in Table 1. Within the experimental error the slopes of all four isotherms gave the value of unity, indicating a first-order process. The result of the isothermal technique analysis agreed with that of the coverage study for the CO_2 product. In addition, these four isotherms were obtained with more than one order of magnitude change in coverage. No evidence of any coverage dependence of k was observed. Hence these *straight* isotherms were indicative of the rate constant to be coverage independent, or its degree of dependence was so negligibly small that it was perfectly valid to assume the rate constant to be coverage independent.

Two different techniques were used to determine the activation energy of the CO_2 product: the heating rate variation method and the method of desorption isosteres. The detailed analysis of the heating rate variation method was described previously (*16*). In this method $\ln(N_p)$ and $\ln(\beta/T_p{}^2)$ were plotted, respectively, as a function of the reciprocal peak temperature (T_p). N_p is the maximum desorption rate and β is the linear heating rate. The activation energy was determined from the slopes of these plots. The activation energy values of the CO_2 product was calculated to be 31.89 and 31.87 kcal/mole from the plots of $\ln(N_p)$ and $\ln(\beta/T_p{}^2)$, respectively.

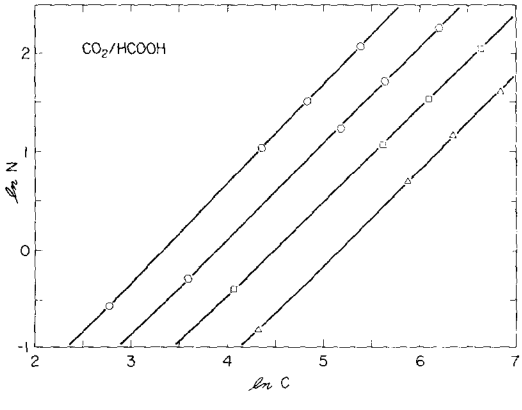

FIG. 4. Isothermal analysis for the CO_2/HCOOH(RT) product peak. (a) 478°K; (b) 470°K; (c) 463°K; (d) 455°K.

TABLE 1

Reaction Order Determination from Isothermal Plots

Isotherm (°K)	Reaction order measured from slope of isothermal plot
478	1.01
470	0.98
463	0.96
455	0.97

The other technique was related to constant surface coverage. From Eq. (2),

$$N = \nu_n \exp\left(\frac{-E}{RT}\right) C^n, \qquad (2)$$

where ν_n is the preexponential factor and E is the activation energy one obtains the following expression:

$$\ln(N) = \ln(\nu_n) + n\ln(C) - E/RT \qquad (3)$$

In some special cases, the preexponential factor will be coverage dependent (*17*), but at fixed surface coverage, the whole term $(\ln(\nu_n) + n\ln(C))$ becomes a constant. Hence, a plot of $\ln(N)$ as a function of reciprocal temperature should yield a straight line with the slope representing the activation energy. This technique has the same advantage as the heating rate variation method, i.e., no assumption of the reaction order is required. Figure 5 shows a plot of $\ln(N)$ versus the reciprocal temperature for the CO_2 product. The activation energy was found to be 33.3 kcal/mole.

DISCUSSION

Dehydrogenation was the *sole* reaction path for the catalytic decomposition of formic acid on a clean Cu(110) surface. The results indicated that formic acid was dissociatively adsorbed on a Cu(110) surface forming a stable formate surface intermediate ($HCOO_{(a)}$) and adsorbed hydrogen

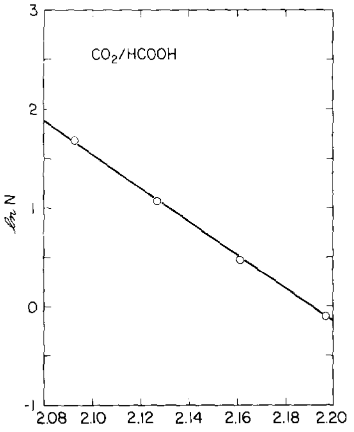

FIG. 5. Determination of the activation energy of the $CO_2/HCOOH$ peak by plotting ln(N) versus the reciprocal temperature at constant coverage.

which desorbed directly below room temperature. When the sample was flashed above 400°K, the adsorbed formate surface intermediates decomposed, giving off carbon dioxide and hydrogen. The entire reaction sequence was therefore as follows:

$$HCOOD_{(g)} \rightarrow HCOO_{(a)} + D_{(a)}$$

$$2D_{(a)} \rightarrow D_{2(g)}$$

$$HCOO_{(a)} \rightarrow CO_{2(g)} + H_{(a)} \qquad \text{(slow)}$$

$$2H_{(a)} \rightarrow H_{2(g)} \qquad \text{(fast)}$$

This mechanism was also supported by the observed product stoichiometries. It was interesting to note that the $H_2(\gamma)/HCOOH$ peak was about 50° lower than the H_2/H binding state observed on the Cu(110) surface (*18*). This low temperature desorption of the $H_2(\gamma)$ peak was probably induced by the formate ions, but the nature of this interaction is not exactly understood at this time. Additionally, the magnitude of the $H_2(\gamma)/HCOOH$ peak was only about 70% of the $H_2(\beta)$ peak. This difference may be due to a competition for sites between $H_{(a)}$ and the absorbed formate, resulting in the displacement of some of the $H_{(a)}$ formed from HCOOH upon adsorption.

The formation of $CO_2/HCOOD$ and $H_2/HCOOD$ products shown in the decomposition steps were governed by the same rate-limiting step. Figure 6 shows the comparison of the normalized desorption spectra of CO_2 and H_2; the desorption spectra coincided exactly. The isothermal technique and coverage variation method showed a first-order process for the formation of carbon dioxide. This result, coupled with the fact that there is no binding state for CO_2 on Cu(110) surface (*19*), indicated the decomposition of the $HCOO_{(a)}$ surface intermediate was the rate-limiting step for the CO_2 product. Furthermore, the recombination of the hydrogen atoms was a relatively fast process in the high temperature region. Hence, the formation of both the $CO_2(\beta)/HCOOD$ and $H_2(\beta)/HCOOD$ products were governed by the decomposition of the $HCOO_{(a)}$ surface intermediate.

The measured activation energy was used to generate a first-order theoretical spectrum to fit the CO_2 peak. The activation energy required for the decomposition of the absorbed formate species was determined by the heating rate variation method and a constant surface coverage technique. Within experimental discrepancy, the values measured in these two techniques agreed with each other as the difference was less than 5%. Figure 7 shows a theoretically simulated spectrum with an activation energy of 31.87 kcal/mole and a preexponential factor of 9.4×10^{13} sec^{-1}. This generated spectrum fits the CO_2 peak except

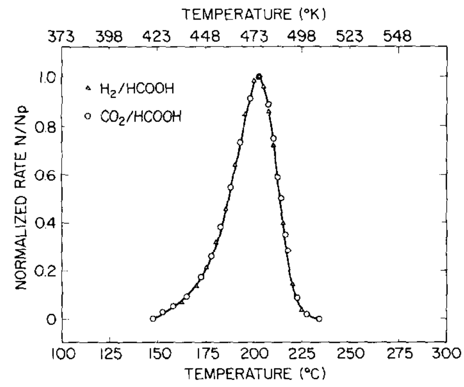

FIG. 6. Comparison of the normalized spectra of $CO_2/HCOOH$ and $H_2/HCOOH$ products.

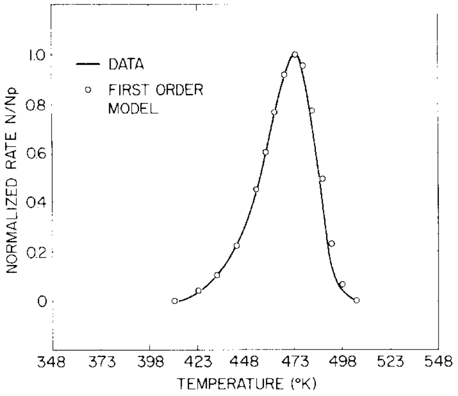

FIG. 7. Computer simulation to fit the $CO_2/HCOOH$ product spectrum. First-order process activation energy was 31.87 kcal/mole. Preexponential factor was 9.4×10^{13} sec^{-1}. Heating rate was 4.7 $ksec^{-1}$.

for a very slight discrepancy at the high temperature edge.

There was a significant difference between the preexponential factor for the decomposition of the adsorbed formate species on a Cu(110) surface and that on a carburized nickel surface (*12*). This difference may have been due to different molecular orientation of the chemisorbed formate species. Formic acid decomposition on Ni(110) (2 × 1)C and Ni(110) (4 × 5)C surfaces was studied by McCarty and Madix (*12, 13, 20*). The activation energy and preexponential factor were found to be 25 kcal/mole and 2×10^{12} sec^{-1}, respectively. The decomposition of the formate species $HCOO_{(a)}$ was also found to be the rate limiting step.

In any event, the low value of the preexponential factor observed on the carburized Ni surface was rationalized by the loss of degrees of freedom in the transition state. On Cu(110) the decomposition of the same formate species was also the rate-limiting step. However, the preexponential factor was larger by more than one order of magnitude. This difference in the preexponential factor indicated that the adsorption state of the formate species on a copper surface may be different from that on a carburized nickel surface possessing less entropy. If it is postulated that the formate species is chemisorbed on the copper surface through the two oxygen atoms as shown below, then it is reasonable to believe that the transition state might show an

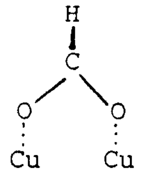

increase in entropy via the loosening of the bonds of the complex. Hence, the preexponential factor of $10^{13.9}$ sec^{-1} observed for the formate decomposition on the copper surface seems reasonable.

The molecular orientation of chemisorbed formate on evaporated copper films was studied by Ito and Suetaka (*21*) using infrared reflection spectroscopy. The investigators reported the observation of the strong infrared adsorption band at 1360 cm^{-1} which was assigned to the symmetric OCO stretching vibration and the absence of the antisymmetric vibration at 1590 cm^{-1}. This results, coupled with the earlier transmission study (*22*), suggested that the chemisorbed formate molecules were oriented almost vertically on the copper surface, having the oxygen atoms bonded to the surface site. These results lend support to the above transition state model. Furthermore, in the oxidation of formaldehyde on a Cu(110) surface, $H_2C^{16}O$ was observed to exchange with preadsorbed ^{18}O to form $H_2C^{18}O$ (*18*). This result suggested that the ^{16}O atom of the $H_2C^{16}O$ molecule was bonded to the surface allowing the carbon atom to pick up a ^{18}O surface atom to exchange with the ^{16}O atom. It was also observed that the $H_2C^{16}O$ reacted with a surface ^{18}O atom to form a stable $HC^{16}O^{18}O$ intermediate, further supporting the suggested chemisorbed model for the formate on the Cu(110) surface mentioned above.

The formic acid decomposition products observed in the current study agreed with those reported in the literature (*1–9*). However, only the results of three investigators for the activation energy for the decomposition of formic acid on copper catalyst (*4, 6, 9*) agreed with that found in this work on a single crystal surface. In the present study the leading edge of the CO_2 spectrum indicated that the formate species started to decompose around 400°K, in agreement with that reported by Joyner and Roberts (*11*). However, the activation energy for the decomposition of the formate ion reported by Joyner and Roberts was calculated by assuming a value of 10^{13} for the preexponential factor. If this assumed value was replaced by the preexponential factor of $10^{13.9}$ measured in the present study, the activation energy became 29.5–33.1 kcal/mole. These values were in better agreement with the presently calculated activation energy which was determined with neither the assumption of a reaction order nor the assignment of a preexponential factor value. Furthermore, in a recent study of the oxidation of methanol on a Cu(110) surface (*23*), an activation energy of 31.0 ± 1.0 kcal/mole was measured for the CO_2 product deriving from the decomposition of an adsorbed HCOO surface intermediate. A preexponential factor of 8×10^{13} sec^{-1} was also reported; this value agreed with the present result of 9×10^{13} sec^{-1}.

It has also been suggested (*12, 13*) that the nickel carbide surface may behave more like copper than nickel because of the possible filling of the d-band of the nickel atom by the valence electron of carbon. Photoemission and optical data (*24, 25*) showed that the nickel d-band density of the states at the Fermi level was sharply attenuated with the presence of surface carbon; the reason for this attenuation was not exactly understood. Qualitatively the results obtained on Ni(110) (2 × 1)C and Cu(110) were similar, in that the formate intermediate dominated the mechanism and the surface formic anhydride was suppressed. The 5 to 6 kcal/mole difference in the activation energy observed for the carburized nickel surface and for the Cu(110) surface indicated quantitative differences, however. A careful inspection of the CO_2/HCOOH spectrum observed on the carburized nickel surface showed a high temperature shoulder at the same temperature as the peak position of the CO_2 product observed on the clean Cu(110) surface in the present study. Previously, the CO_2 product spectrum from the nickel carbide surface was fitted with a three-state model consisting of three first-order binding states (β_1, β_2, and β_3). The rate parameters for the β_2 and β_3 states and the relative coverage of the three states were adjusted over a wide range to fit the flash curves. In fact, when the Arrhenius parameters of the β_2 state were replaced by those measured for the CO_2 product in the present study and a relative coverage of 10 : 4 : 3 was used for $\beta_1 : \beta_2 : \beta_3$, an equally adequate fitting was obtained, as shown in Fig. 8. This fit, coupled with the matching of the shoulder of the CO_2 peak observed on the carburized nickel surface to the CO_2 peak observed on the Cu(110) surface, sug-

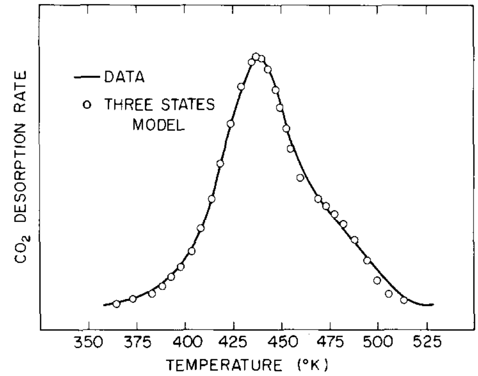

Fig. 8. A three-states model to fit the CO_2/HCOOH product spectrum observed on the carburized nickel surface.

State	Activation energy (kcal/mole)	Preexponential factor (sec^{-1})
β_1	25.0	2×10^{12}
β_2	31.87	9.4×10^{13}
β_3	24.5	4.0×10^{11}

Relative coverage $\beta_1 : \beta_2 : \beta_3$ was 10 : 4 : 3. The information of the β_1 and β_3 was obtained from Ref. (*13*). The experimental data were obtained from Ref. (*13*). All three states were first-order process.

gested that one decomposition pathway on the nickel carbide surface quantitatively duplicated that observed on copper. In view of these facts it appears that certain features of the nickel carbide surface produce chemical reactivity for formate decomposition identical to copper. Unfortunately, the addition of surface carbon on nickel resulted in the formation of islands of surface carbon rather than randomly substitutional nickel carbide surface (*26*) so that this surface could not be directly compared to the random Ni/Cu alloy surfaces reported elsewhere (*27*).

SUMMARY

The formic acid molecule decomposed on the Cu(110) surface to form carbon dioxide and hydrogen *solely*. The dissociation of the parent molecule occurred below room temperature leaving a stable formate $HCOO_{(a)}$ as the surface intermediate. This formate species was held on the surface until above 400°K when it started to decompose forming the CO_2 and H_2 product. The decomposition of the adsorbed formate governed the rates of the CO_2 and H_2 formation. The activation energy and the preexponential factor for the decomposition of the formate was determined to be 31.9 kcal/mole and $10^{13.9}$ sec^{-1}, respectively. This measured preexponential value was reasonable quantity in view of results of the infrared study of the chemisorbed formate on evaporated copper films (*21*).

A comparison of the catalytic properties of the Cu(110) surface with those of the Ni(110) (2 × 1)C surface indicated that the nickel carbide surface did not exactly behave chemically like a copper surface, though qualitative features of the decomposition on both surfaces were identical.

ACKNOWLEDGMENTS

The authors wish to acknowledge support of this work by the National Science Foundation grant number NSF-DMR-74-22230-AO1 through the Solid State Electronics Laboratories, Stanford Electronic Laboratories, Stanford University. Professor Madix would also like to express his gratitute to the Humboldt Foundation for support during preparation of this manuscript.

REFERENCES

1. Rienacker, G., and Hildebrandt, H., *Z. Anorg. Chem.* **248,** 52 (1941).
2. Schwab, G.-M., and Schwab-Agallidis, E., Ber. **76,** 1228 (1943).
3. Schwab, G.-M. and Schwab-Agallidis, E., *Naturwissenschaften* **31,** 322 (1943).
4. Dowden, D. A., and Reynolds, P. W., *Disc. Faraday Soc.* **8,** 184 (1950).
5. Crocker, A. J., and Robertson, A. J. B., *Trans. Faraday Soc.* **54,** 931 (1958).
6. Tamaru, K., *Trans. Faraday Soc.* **55,** 824, 1191 (1959).
7. Fuderer-Leutic, P., and Brihta, I., *Croat. Chim. Acta* **31,** 75 (1959).
8. Ruka, R. J., Brockway, L. O., and Boggs, J. E., *J. Amer. Chem. Soc.* **81,** 2930 (1959).
9. Duell, M. J., and Robertson, A. J. B., *Trans. Faraday Soc.* **57,** 1416 (1961).
10. Inglis, H. S., and Taylor, D., *Inorg. Phys. Theor. J. Chem. Soc.* A2985 (1969).
11. Joyner, R. W., and Roberts, M. W., *Proc. R. Soc. London* **A350,** 107 (1976).
12. McCarty, J., and Madix, R. J., *J. Catal.* **38,** 402 (1975).
13. McCarty, J., Ph.D. Dissertation, Stanford University, 1974.
14. Levi, R. B., and Boudart, M., *Science* **181,** 547 (1973).
15. McCarty, J., Falconer, J., and Madix, R. J., *J. Catal.* **31,** 316 (1973).
16. Falconer, J., and Madix, R. J., *Surface Sci.* **48,** 393 (1975).
17. Abbas, N., and Madix, R. J., *Surface Sci.* **62,** 739 (1977).
18. Wachs, I. E., and Madix, R. J., *Surface Sci.* **84** (1979) in press.
19. Ying, D. H. S., and Madix, R. J., unpublished data.
20. McCarty, J., Falconer, J., and Madix, R. J., *J. Catal.* **31,** 316 (1973).
21. Ito, M., and Suetaka, W., *J. Phys. Chem.* **79,** 1190 (1975).
22. Hirota, K., and Nakai, Y., *Nihon Kagaku Zashi* **80**(7), 700 (1959).
23. Wachs, I. E., and Madix, R. J., *J. Catal.* **53,** 208 (1978).
24. Seib, D. H., Ph.D. Dissertation, Stanford University, 1969.

25. Demuth, J., private communication.

26. Abbas, N., and Madix, R. J., unpublished data. When the surface carbide was formed on Ni(110), a decrease of the explosive CO_2 peak and the growth of the CO_2 peak due to decomposition on the nickel carbide were observed simultaneously. This was ascribed to the formation of islands of surface carbide.

27. Ying, D. H. S., and Madix, R. J., *J. Inorg. Chem.* 7, 1103 (1978).